Journal of Zhejiang University SCIENCE A
ISSN 1673-565X (Print); ISSN 1862-1775 (Online)
www.zju.edu.cn/jzus; www.springerlink.com
E-mail: jzus@zju.edu.cn

Behaviour of cold-formed stainless steel beams at elevated temperatures*

Ju CHEN, Wei-liang JIN†‡

(*Department of Civil Engineering, Zhejiang University, Hangzhou 310058, China*)

†E-mail: Jinwl@zju.edu.cn

Received Apr. 15, 2008; revision accepted June 10, 2008

Abstract: A study of the behaviour of constructional cold-formed stainless steel beams at elevated temperatures was conducted in this paper. An accurate finite element model (FEM) for stainless steel beams was developed using the finite element program ABAQUS. Stainless steel beams having different cross-sections were simulated in this study. The nonlinear FEM was verified against the experimental results. Generally, the developed FEM could accurately simulate the stainless steel beams. Based on the high temperature stainless steel material test results, a parametric study was carried out on stainless steel beams at elevated temperatures using the verified FEM. Both high strength stainless steel EN 1.4462 and normal strength stainless steel EN 1.4301 were considered. A total of 42 stainless steel beams were simulated in the parametric study. The effect of temperatures on the behaviour of stainless steel beams was investigated. In addition, a limiting temperature for stainless steel beams was also proposed.

Key words: Elevated temperatures, Finite element model (FEM), Fire, Stainless steel beams
doi: 10.1631/jzus.A0820285 **Document code:** A **CLC number:** TU5

INTRODUCTION

Cold-formed stainless steel members are being increasingly used in architectural and structural applications because of the desirable features of the material—corrosion resistance, durability, easy maintenance, pleasing appearance, recyclability and fire resistance. A cold-formed hollow section is formed by rolling an annealed flat strip into a circular hollow section, which is then welded at the edges. The process is completed by further rolling into a square or rectangular hollow section (SHS or RHS). This process of forming by cold-working leads to a considerable enhancement of the material properties of the annealed steel, especially in the corner portion of the cross-section. Normally the cold-forming operation increases the yield point and tensile strength and at the same time decreases the ductility. More economical designs can be achieved by taking into account the enhancement of the material properties due to cold-working.

Previous research concentrated mostly on the behaviour and design of stainless steel members at normal room temperature (Young and Liu, 2003; Gardner and Nethercot, 2003; Rasmussen *et al.*, 2004; Real and Mirambell, 2005; Gardner, 2005; Ashraf *et al.*, 2005). However, research into stainless steel at elevated temperatures is rather limited. Gardner (2007) and Ala-Outinen and Oksanen (1997) conducted a series of concentric compression tests on rectangular 40 mm×40 mm×4 mm hollow sections cold-formed from austenitic stainless steel of type Polarit (conforming to material numbers EN 1.4301 and AISI 304). Gardner and Baddoo (2006) conducted a series of tests on six grade 1.4301 stainless steel columns and four fire tests on grade 1.4301 stainless steel beams. The tested four beams include one RHS beam (with a Class 1 cross-section) formed by two cold-rolled channels (welded tip-to-tip), one I-section beam (with a Class 4 cross-section) formed by two cold-rolled

‡ Corresponding author

* Project supported by the Hi-Tech Research and Development Program (863) of China (No. 2006AA04Z422) and the Post-doctoral Fund of Zhejiang Province (No. 113000-X80703), China

channels (welded back-to-back), and two I-section beams of constant (Class 1) cross-section. Gardner and Ng (2006) investigated the temperature development in structural stainless steel sections exposed to fire. Therefore there is still a lack of information on the behaviour of cold-formed stainless steel beams at elevated temperatures. With heightened emphasis now being placed on the performance of structures at elevated temperatures (Bailey, 2004), and an increasing trend towards the use of bare steelwork (Wong *et al*., 1998), it is important to investigate the behaviour of cold-formed stainless steel members at elevated temperatures.

It can be quite costly and time-consuming for experimental investigation, therefore numerical methods have been used in the area of steel structural fire resistant design in recent years. The finite element program ABAQUS (2004) has been widely used to investigate the behaviour of cold-formed stainless steel members at normal room temperature. In addition, ABAQUS has also been used to investigate cold-formed steel members at elevated temperatures (Feng *et al*., 2003; Lee and Mahendran, 2004). Therefore the finite element program ABAQUS is used to simulate cold-formed stainless steel beams at elevated temperatures in this study.

FINITE ELEMENT MODEL

General

In this study the stainless steel beams tested by Zhou and Young (2005) were firstly simulated to verify the finite element model (FEM). The FEM was developed according to the experimental setup, as shown in Fig.1. Load-displacement nonlinear analysis was performed in the analysis. In addition, careful attention was given to the choice of the element type and mesh size to combine a high level of numerical accuracy and stability with optimum computational efficiency.

Finite element type and mesh

A four-node doubly curved shell element with reduced integration and hourglass control (S4R5) was used in the simulation of beams. The element has five degrees of freedom per node. In the simulation of beams, only half of the specimen was modeled for symmetry. In order to choose the finite element mesh that provides accurate results with minimum computational time, convergence studies were conducted. It was found that an approximate 10 mm×10 mm (length by width) ratio provides adequate accuracy in modeling the beams with a fine mesh in the corner portion, as shown in Fig.2.

(a)

(b)

Fig.1 Comparison of (a) experimental specimen and (b) FEM for beam specimen N40-40-2

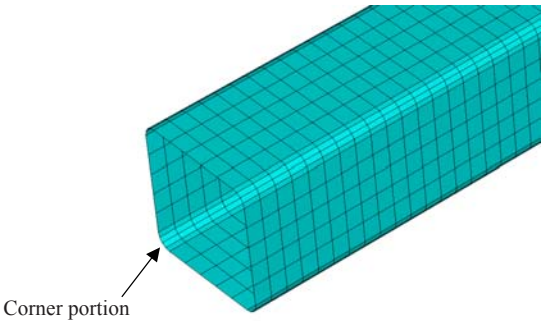

Fig.2 Finite element mesh of beam specimen N40-40-2

Boundary conditions and load application

Following the test procedure the beam was four-point loaded. In the FEM, the support plate was modeled as a rigid surface whose motion is governed by the reference point. The reference point of the support plate was restrained against x, y and z directions displacement as well as y- and z-axes rotation but was free to rotate about the x-axis. The loading

plate was also modeled as a rigid surface. The reference point of the loading plate was restrained against x and z directions displacement as well as y- and z-axes rotation but was free to move in y direction and rotate about the x-axis. The constraint between the loading/support plate and specimen was simulated using a contact surface, as shown in Fig.3. The web stiffener plates which stiffen the section at the load and support points were simulated by increasing the approximate 70% thickness of the elements at the corresponding parts. Thus local failure at the loading and support points was prevented. The load was applied at the reference point of the loading plate. The nonlinear geometry parameter (NLGEOM) was included to deal with the large displacement analysis.

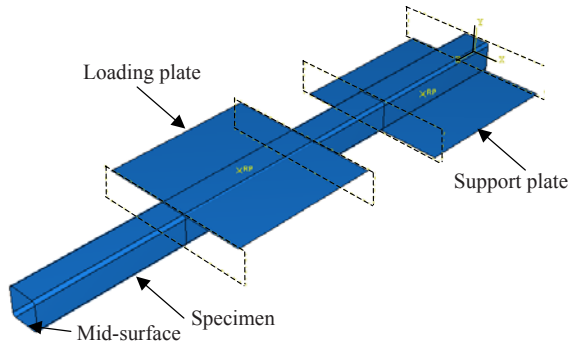

Fig.3 Boundary conditions and load application of finite element model for specimen N40-40-2

Material modeling

In the FEM the measured stress-strain curves were used. The static stress-strain curves were first obtained by knowing the static loads near to the 0.2% proof stress and ultimate stress. Since the analysis involves large inelastic strains, the nominal (engineering) static stress-strain curve was converted to a true stress and plastic true strain curve. The true stress and plastic true strain were specified in ABAQUS (2004). Another important issue is thermal expansion. Stainless steel expands more than carbon steel at elevated temperatures. However, the specimens investigated in this study are free from thermal expansion and therefore it is not included.

VERIFICATION OF FINITE ELEMENT MODEL

The stainless steel beams tested by Zhou and Young (2005) were modeled in this study. The measured cross-section dimensions and material properties reported in Zhou and Young (2005) were incorporated in the FEM. The ultimate moments of the stainless steel beams obtained from finite element analysis (FEA) ($M_{\text{u-FEA}}$) are compared with the test results ($M_{\text{u-TEST}}$) presented by Zhou and Young (2005) in Table 1. The test specimens are labeled such that the steel types and cross-section dimensions could be identified from the label. For example, the labeled 'N100-50-2' defines the specimen having normal strength material and nominal overall depth of the web of 100 mm, overall flange width of 50 mm, and thickness of 2.0 mm. The mean values of the ultimate moment ratio ($M_{\text{u-TEST}}/M_{\text{u-FEA}}$) are 0.97 with the corresponding coefficients of variation (COV) 0.025. A maximum difference in ultimate moments of 7% was observed between test and numerical results for a beam specimen of N120-60-2. The comparison indicates that the ultimate moments of beams predicted by the FEA are accurate. In addition, the load vs mid-span deflection curve obtained from the FEA was compared with test results of specimen H40-40-2, as shown in Fig.4. It is also shown that the FEA results of the load vs mid-span deflection curve agree well with the test results.

Table 1 Comparison of FEA results with stainless steel beam test results

Specimen	$M_{\text{u-TEST}}$ (kN·m)	$M_{\text{u-FEA}}$ (kN·m)	Comparison $M_{\text{u-TEST}}/M_{\text{u-FEA}}$
N40-40-2	2.35	2.42	0.97
N40-40-4	5.11	5.37	0.95
N80-80-2	6.64	6.94	0.96
N80-80-5	24.78	24.89	1.00
N100-50-2	8.81	9.19	0.96
N100-50-4	21.28	22.73	0.94
N120-60-2	10.25	11.03	0.93
N120-60-4	34.09	33.63	1.01
H40-40-2	3.45	3.45	1.00
H50-50-1.5	3.48	3.62	0.96
H150-150-3	31.68	32.85	0.96
H150-150-6	108.60	111.38	0.98
H140-80-3	33.97	35.80	0.95
H160-80-3	39.36	41.07	0.96
H200-110-4	80.15	80.20	1.00
Mean	0.97	*COV**	0.025

**COV*: Coefficients of variation

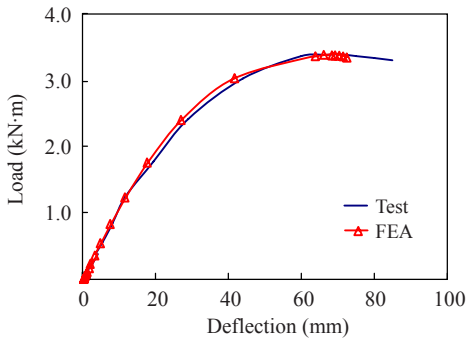

Fig.4 Comparison of moment vs mid-span deflection curves obtained from test results of specimen H40-40-2 with FEA results

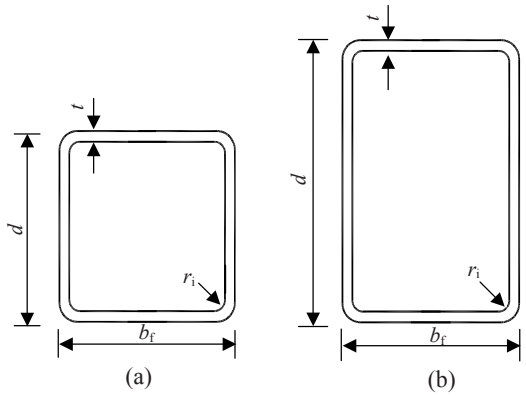

Fig.5 Definition of symbols. (a) Square hollow section; (b) Rectangular hollow section

PARAMETRIC STUDY

The verification showed that the FEM of stainless steel beams at elevated temperatures was reasonably accurate. Hence parametric study was carried out to investigate the behaviour of stainless steel beams at elevated temperatures. Cold-formed high strength stainless steel structural members have been increasingly used in structural applications (Young and Liu, 2005). However, there is no data available on the material behavior of cold-formed high strength stainless steel members at elevated temperatures. Therefore the behaviour of high strength stainless steel beams was also investigated in this paper. Three kinds of beam sections, namely 50-100-2, 40-40-2, 100-50-2, are investigated in the parametric study. The cross-section dimensions are shown in Table 2 using the symbols defined in Fig.5. Those sections are chosen so that both thin-walled and compact sections of rectangular and square sections are included.

An experimental investigation of the mechanical properties of high strength and normal strength stainless steel at elevated temperatures has been conducted by Chen and Young (2006). The test program included two stainless steel grades of EN 1.4462 and EN 1.4301 with nominal yield strengths of 793 MPa and 398 MPa, respectively. The yield strength ($f_{y,T}$) and elastic modulus (E_T) of stainless steel grades of EN 1.4462 and EN 1.4301 at elevated temperatures were presented in Table 3. In the simulation of beams at elevated temperatures, the stress-strain curves of both high and normal strength stainless steel obtained by Chen and Young (2006) were used. The material behaviour provided by ABAQUS (2004) allows a multi-linear stress-strain curve to be used. The first part of the multi-linear curve represents the elastic part up to the proportional limit stress with measured elastic modulus and Poisson's ratio. In this study, the Poisson's ratio is taken as 0.3 under fire conditions. Generally, the Poisson's ratio is assumed to be independent of temperature (Kaitila, 2002; Zha, 2003). The labeling system for the stainless steel beams at elevated temperatures is similar to that used for normal room temperature. In the parametric study, the temperature is also considered in the labeling system. Therefore, the letter "T" is added in the labels. For example, the label "H40-40-2T22" defines the specimen of H40-40-2 at a temperature of 22 °C, where "T" indicates the temperature of the specimen followed by the value of the temperature in degree Celsius. The temperature values chosen in the parametric study are 22, 320, 450, 550, 660, 760 and 960 °C.

Table 2 Dimensions for specimens of parametric study*

Specimen	Web d (mm)	Flange b_f (mm)
H50-100-2	52.0	102.0
H40-40-2	42.0	42.0
H100-50-2	102.0	52.0
N50-100-2	52.0	102.0
N40-40-2	42.0	42.0
N100-50-2	102.0	52.0

*The thickness t is 2.0 mm; the radius r_i is 2.0 mm; the length L is 1440 mm

DISCUSSION

The ultimate moment of high strength and normal strength stainless steel beams ($M_{u,T}$) obtained from the

FEA are shown in Tables 4 and 5, respectively. In addition, the moment vs mid-span deflection curves of specimen series H40-40-2 and N40-40-2 were also plotted, as shown in Figs.6a and 6b, respectively. It is shown that the moment vs mid-span deflection curves at elevated temperatures are generally similar to those at normal room temperature. When temperature increases, the mid-span deflection corresponding to the maximum moment also increases for temperatures lower than 660 °C, which means that the deformation capacity of stainless steel beams increases. However, the deformation capacity of stainless steel beams decreases when the temperature is higher than 660 °C.

The load ratio of the ultimate moment of stainless steel beams was plotted against different temperatures in Figs.7a and 7b for high strength stainless steel and normal strength stainless steel, respectively. The load ratio is defined as the maximum moment of a beam at elevated temperatures ($M_{u,T}$) compared to that at normal room temperature ($M_{u,normal}$), as shown in Eq.(1):

$$\text{Load ratio}=M_{u,T}/M_{u,normal}. \quad (1)$$

It is shown that the specimen lost approximately 30% of its strength when the temperature reached 450 °C. For high and normal strength stainless steel beams, the load ratio decreases rapidly when the temperature reaches 660 °C and 550 °C, respectively. For conservatism, 550 °C was considered as the limiting temperature for both high and normal strength stainless steel beams.

Table 3 Material properties of stainless steel EN 1.4462 and EN 1.4301 at elevated temperatures used in the parametric study

Temperature (°C)	Stainless steel grade EN 1.4462		Stainless steel grade EN 1.4301	
	E_T (MPa)	$f_{y,T}$ (MPa)	E_T (MPa)	$f_{y,T}$ (MPa)
22	227000	731	187000	398
320	162078	554	193732	278
450	157992	532	177837	270
550	156600	499	168300	237
660	145961	386	161194	208
760	92843	259	107338	142
960	13620	23	63580	46

Table 4 Ultimate moments for high strength stainless steel beams obtained from the FEA

Specimen	$M_{u,T}$ (kN·m)	Specimen	$M_{u,T}$ (kN·m)	Specimen	$M_{u,T}$ (kN·m)
H50-100-2T22	6.6	H40-40-2T22	3.4	H100-50-2T22	14.6
H50-100-2T320	5.0	H40-40-2T320	2.7	H100-50-2T320	11.5
H50-100-2T450	4.9	H40-40-2T450	2.5	H100-50-2T450	11.1
H50-100-2T550	4.8	H40-40-2T550	2.4	H100-50-2T550	10.4
H50-100-2T660	3.8	H40-40-2T660	1.9	H100-50-2T660	7.8
H50-100-2T760	2.6	H40-40-2T760	1.1	H100-50-2T760	4.8
H50-100-2T960	0.3	H40-40-2T960	0.1	H100-50-2T960	0.6

Table 5 Ultimate moments for normal strength stainless steel beams obtained from the FEA

Specimen	$M_{u,T}$ (kN·m)	Specimen	$M_{u,T}$ (kN·m)	Specimen	$M_{u,T}$ (kN·m)
N50-100-2T22	4.1	N40-40-2T22	2.0	N100-50-2T22	8.9
N50-100-2T320	3.5	N40-40-2T320	1.4	N100-50-2T320	6.4
N50-100-2T450	3.4	N40-40-2T450	1.3	N100-50-2T450	6.2
N50-100-2T550	3.0	N40-40-2T550	1.2	N100-50-2T550	5.5
N50-100-2T660	2.9	N40-40-2T660	1.1	N100-50-2T660	5.2
N50-100-2T760	1.8	N40-40-2T760	0.7	N100-50-2T760	3.4
N50-100-2T960	1.0	N40-40-2T960	0.2	N100-50-2T960	1.4

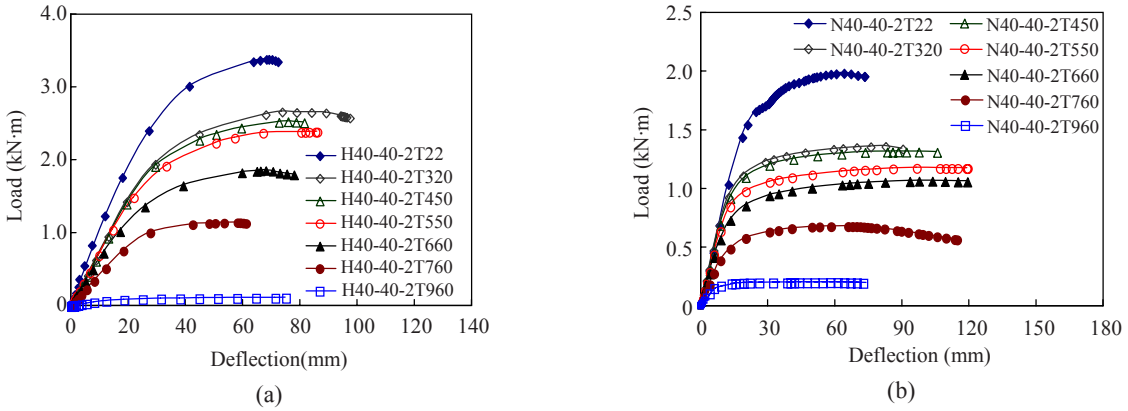

Fig.6 Moment vs mid-span deflection curves of specimen series (a) H40-40-2 and (b) N40-40-2 at elevated temperatures

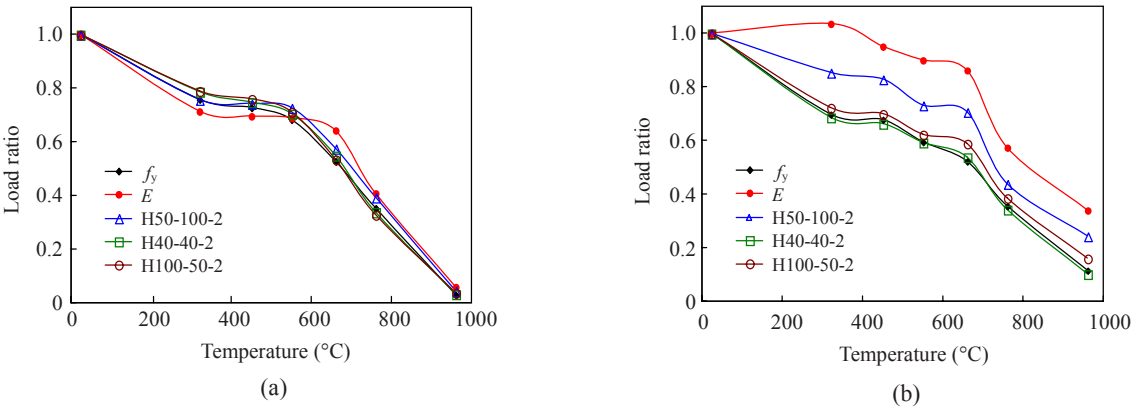

Fig.7 Load ratio of (a) high strength and (b) normal strength stainless steel beams at elevated temperatures

The reduction ratio of yield strength (f_y) and elastic modulus (E) were also plotted in Fig.7 for comparison. It is shown that for high strength stainless steel, the load ratio curves are similar to the reduction ratio curves of material properties. For normal strength stainless steel, the load ratio curves are generally between the reduction ratio curves of yield strength and elastic modulus. The reduction ratio curves of elastic modulus could be considered as upper boundary while the reduction ratio curves of yield strength could be considered as lower boundary.

CONCLUSION

This paper focuses on the behaviour of stainless steel beams at elevated temperatures. An accurate FEM was developed and verified against experimental results. It is shown that the FEM can simulate the stainless steel beams accurately. Therefore a parametric study was conducted using the verified FEM. Six series of stainless steel beams (42 specimens) having different cross-sectional dimensions and material properties were investigated. It is shown that the deformation capacity of stainless steel beams increases when the temperature increases in the range of 22~660 °C. However, the deformation capacity of stainless steel beams decreases when the temperature increases in the range of 660~960 °C. Based on the investigation, a limiting temperature of 550 °C for both high and normal strength stainless steel beams was suggested in this study. For high strength stainless steel beams, the load ratio curves are similar to the reduction ratio curves of material properties. For normal strength stainless steel beams, the reduction ratio curves of elastic modulus could be considered as upper boundary while the reduction ratio curves of yield strength could be considered as lower boundary.

References

ABAQUS, 2004. Analysis User's Manual. Version 6.5. ABAQUS, Inc.

Ala-Outinen, T., Oksanen, T., 1997. Stainless Steel Compression Members Exposed to Fire. VTT Research Notes, Technical Research Center of Finland, Espoo, Finland.

Ashraf, M., Gardner, L., Nethercot, D.A., 2005. Strength enhancement of the corner regions of stainless steel cross-sections. *Journal of Constructional Steel Research*, **61**(1):37-52. [doi:10.1016/j.jcsr.2004.06.001]

Bailey, C., 2004. Structural fire design: core or specialist subject. *Structural Engineer*, **82**(9):32-38.

Chen, J., Young, B., 2006. Stress-strain curves for stainless steel at elevated temperatures. *Engineering Structures*, **28**(2):229-239. [doi:10.1016/j.engstruct.2005.07.005]

Feng, M., Wang, Y.C., Davies, J.M., 2003. Structural behaviour of cold-formed thin-walled short steel channel columns at elevated temperatures. Part 2: design calculations and numerical analysis. *Thin-Walled Structures*, **41**(6): 571-594. [doi:10.1016/S0263-8231(03)00003-X]

Gardner, L., 2005. The use of stainless steel in structures. *Progress in Structural Engineering and Materials*, **7**(2):45-55. [doi:10.1002/pse.190]

Gardner, L., 2007. Stainless steel structures in fire. *Proceedings of the Institution of Civil Engineers—Structures and Buildings*, **160**(3):129-138. [doi:10.1680/stbu.2007.160.3.129]

Gardner, L., Nethercot, D.A., 2004. Numerical modeling of stainless steel structural components—a consistent approach. *Journal of Structural Engineering*, **130**(10):1586-1601. [doi:10.1061/(ASCE)0733-9445(2004)130:10(1586)]

Gardner, L., Baddoo, N.R., 2006. Fire testing and design of stainless steel structures. *Journal of Constructional Steel Research*, **62**(6):532-543. [doi:10.1016/j.jcsr.2005.09.009]

Gardner, L., Ng, K.T., 2006. Temperature development in structural stainless steel sections exposed to fire. *Fire Safety Journal*, **41**(3):185-203. [doi:10.1016/j.firesaf.2005.11.009]

Kaitila, O., 2002. Finite Element Modeling of Cold-Formed Steel Members at High Temperatures. PhD Thesis, Helsinki University, Finland.

Lee, J.H., Mahendran, M., 2004. Local Buckling Behaviour and Design of Cold-formed Steel Compression Members at Elevated Temperatures. Proceedings of the 4th International Conference on Thin-Walled Structures. Loughborough, England, p.315-322.

Rasmussen, K.J.R., Burns, T., Bezkorovainy, P., 2004. Design of stiffened elements in cold-formed stainless steel sections. *Journal of Structural Engineering*, **130**(11):1764-1771. [doi:10.1061/(ASCE)0733-9445(2004)130:11(1764)]

Real, E., Mirambell, E., 2005. Flexural behaviour of stainless steel beams. *Engineering Structures*, **27**(10):1465-1475. [doi:10.1016/j.engstruct.2005.04.008]

Wong, M.B., Ghojel, J.I., Crozier, D.A., 1998. Temperature-time analysis for steel structures under fire conditions. *Structural Engineering and Mechanics*, **6**(3):275-289.

Young, B., Liu, Y., 2005. Experimental investigation of cold-formed stainless steel columns. *Journal of Structural Engineering*, **129**(2):169-176. [doi:10.1061/(ASCE)0733-9445(2003)129:2(169)]

Zha, X.X., 2003. FE analysis of fire resistance of concrete filled CHS columns. *Journal of Constructional Steel Research*, **59**(6):769-779. [doi:10.1016/S0143-974X(02)00059-7]

Zhou, F., Young, B., 2005. Tests of cold-formed stainless steel tubular flexural members. *Thin-Walled Structures*, **43**(9): 1325-1337.